A MULTI-TONE TESTING TECHNIQUE FOR PRODUCTION CHARACTERIZATION OF MICRO-RESONATORS

Ernest T.-T. Yen[1], Brad Kramer[2], Trevor Tarsi[2], Danielle Griffith[2], and Brian Goodlin[2]
Texas Instruments, [1]Santa Clara / [2]Dallas, USA

ABSTRACT

This work applies a mixed-signal IC production testing technique to perform high-frequency (>1 GHz) micro-resonator characterization on an industry standard ATE (automated test equipment) with an RF subsystem. The implementation is based on observing the change in magnitude and phase of injected multi-tone signals. This μ-resonator ATE technique is capable of extracting the resonance frequency to single-digit ppm accuracy for real-time process monitoring and device pre-screening. Compared to conventional S-parameter measurements on ATEs, this technique is expected to reduce production testing cost by at least 40%.

INTRODUCTION

MEMS testing and packaging account for more than 60% of their total production cost. In a production environment, it usually requires each MEMS device to be characterized and pre-screened at wafer-level to avoid assembly yield loss. For solid-state resonant MEMS devices, common figure of merit parameters (FOMs) include resonance frequencies (f_S/f_P), frequencies at phase inversion (f_R/f_A), impedance at resonances (Z_S/Z_P), quality factors (Q_S/Q_P), effective electromechanical coupling (K^2_{eff}), bulk capacitance (C_0), etc. The capability of being able to measure these FOMs accurately is imperative during technology developing phase as well as for building statistical SPICE models thereafter.

Most capacitive μ-resonator technologies define their operation frequency through lateral dimensions [1-3]. In general, it is uneasy to characterize capacitive μ-resonators prior to encapsulation or wafer-level package because the device performance is sensitive to the ambient pressure variation. It is, therefore, unlikely to perform inline frequency trimming on capacitive μ-resonators and the frequency is usually calibrated after assembling with oscillator circuits. For that reason, capacitive μ-resonators usually operate at a lower frequency range (<100 MHz) to maintain a sufficient coupling [4], and employ fractional-PLLs (phase-locked loops) or capacitor banks for one-time calibration–to correct fabrication errors–and active temperature compensation [2-3].

On the other hand, piezoelectric acoustic resonator technologies such as FBAR (thin-film bulk acoustic resonator) and SMR (solidly mounted resonator) define resonance frequency through the thickness of each constituent layer [5-7]. This thickness-dependence feature allows performing frequency measurement and in-situ trimming alternately at wafer-level. To our knowledge, state-of-the-art frequency accuracy of commercially available acoustic resonator technologies is in the range of ±500 to ±3,000 ppm. Tight process control enables efficient usage of the increasingly crowded RF spectrum

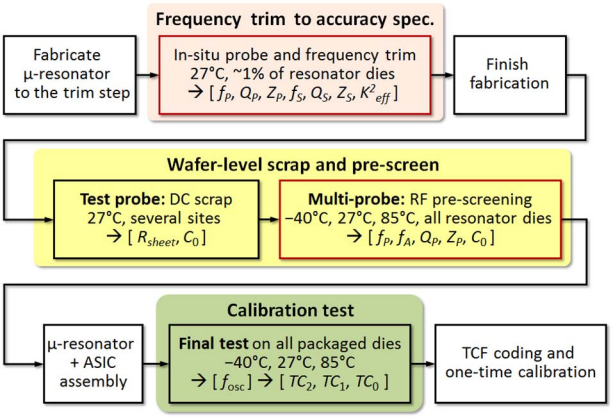

Figure 1: A common production testing flow for μ-resonator based timing systems. The in-situ probe provides process monitoring and control capabilities. Temperature characteristic of each device is derived at wafer-level after multi-temperature testing. This pre-screening also reduces assembly yield loss and final test costs.

[8-9]. Beyond filtering applications, these BAW (bulk acoustic wave) resonators offering high frequency, high quality factor, and small form factor are also suitable for providing precise timing references for standalone clocks and embedded systems [10-12].

Figure 1 shows an example of the μ-resonator production testing flow for high-precision frequency reference applications. Inline RF test-probe is performed right after top electrode deposition and patterning. Due to deposition thickness non-uniformity, the frequency variation across an 8-inch wafer at this step can be as high as ±10,000 ppm (±1%). Several ion-beam frequency trimming steps are performed alternately to reduce this variation to about ±2,000 ppm. Although sufficient for RF filtering applications [5-9], this number needs to be further reduced for timing applications to satisfy the typical specification of ±40 ppm dominated by crystal oscillators. Therefore, the fully-processed wafer is tested again for DC scrap followed by wafer-level multi-probes, during which *all* devices are characterized and pre-screened at different temperatures to extract resonator FOMs and temperature coefficients of frequency (TCFs). Only those dies passing this pre-screen will be used for final assembly.

For most commercially available micromechanical resonators, the frequency stability over temperature and over time (aging) are in the tens of ppm and single-digit-ppm range, respectively. Traditionally, FOMs and TCFs of resonators are extracted from 1-port S-parameter measurement using VNA test cells. However, this test configuration requires the purchase of a production test cell that is unlikely to be utilized by other TI products, driving up test cost. Alternative approaches involve implementing

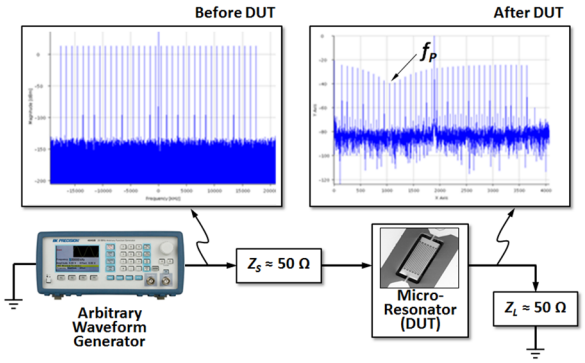

Figure 2: A multi-tone production test configuration. A wideband multi-tone signal covering the entire specified frequency range is applied in the configuration; the μ-resonator results in a dip in magnitude which will be detected at the output.

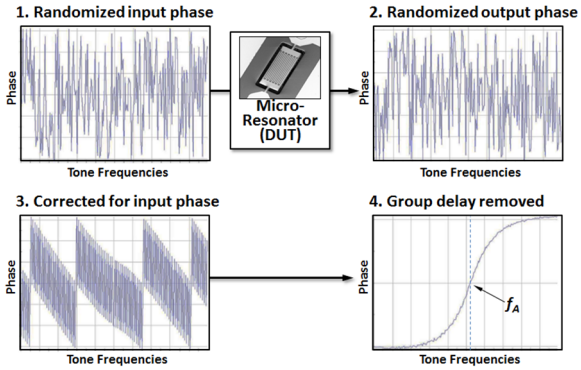

Figure 3: The phase cannot be directly measured due to non-existence of an absolute phase reference. Therefore the multi-tone signal must be corrected to the known input pseudo-random phase.

oscillator circuits, either embedded in the probe tip [13] or a fully-integrated solution [11-12], to directly measure the oscillator's output frequency (with a frequency counter) and phase noise (with a signal source analyzer). Although demonstrated frequency measurement accuracy and precision as good as 0.2 ppm (1σ) [12], this method is unsuitable to extract other FOMs such as the resonance impedance and the quality factor. In addition, the frequency drift during oscillator startup and over temperature also creates major issues. To fulfill these needs and internal low test cost goal, the main challenge is to identify a production test method with measurement repeatability and reproducibility accuracy to single-digit-ppm level.

MULTI-TONE PRODUCTION TEST

Methodology and Testing Setup

The proposed wafer-level test configuration using multi-tone signals for μ-resonator production is shown in Figure 2. An arbitrary waveform generator is used to create a signal that has multiple equally spaced tones of equal amplitude at the input. When these tones pass through a μ-resonator (DUT), it results in a dip in the magnitude response at the parallel resonance frequency f_P. Then, the frequency range of the multi-tone signal is narrowed, centered on this dip and the response is measured again. This process is repeated until a 200-tone signal spaced at 50 kHz is applied to the source. The output magnitude response is then fit to an even-order polynomial to smooth and average out the random noise and quantization noise of the measurement. In order to reduce the peak-to-RMS ratio of the signal created by this arbitrary waveform generator, the phase of each tone is varied in a known pseudo-random sequence (Figure 3). The shape of the magnitude response will vary with different resonator impedances, quality factors, noise from the down conversion process, other excitation modes, etc.

Measuring Frequency and Quality Factor

The parallel resonance f_P can be extracted by finding the minimum of the polynomial near the center of the dip, and Q_P can be derived by dividing f_P by its 3 dB bandwidth. While this quality factor measurement does not follow the standard phase slope definition, it matches to within 0.1% as long as Z_P of the μ-resonator is within specification.

Another critical frequency to measure is the anti-resonance frequency f_A which is defined at where the phase response is zero when transitioning from inductive to capacitive regions. However, the phase cannot be directly measured using multi-tone signals because there is no absolute phase reference between measurements – it depends on when the output signal is captured. The multi-tone signal is therefore corrected to a known input pseudo-random phase and unwound to multiples of 2π when the change in phase is negative. The output phase response is then fit to an odd-order polynomial, where f_A is extracted from the derivative maximum. This procedure is shown in Figure 4. Using the derivative maximum results in a slightly offset value for f_A. However, since the relative drifts remain the same, this multi-tone test method can extract the relative frequency difference at various temperatures ($\Delta f / f_0$) required for the TCF characterization.

Measuring Impedance

The parameter Z_P can also be extracted from the polynomial. As Z_P gets larger, the voltage divider between the DUT impedance and Z_L increases, leading to a deeper dip in the response. Since Z_P is real near the resonance, it can be extracted from the depth of this dip, as given by

$$Z_P = (Z_S + Z_L)\left[\frac{1}{A_V} - 1\right] \quad (1)$$

where Z_S and Z_L are the source and load impedances, and A_V is the amplitude of the signal minimum of the polynomial compared to the amplitude of the response of an on-wafer thru. Ideally, Z_S and Z_L would both be 50 Ω. If the return loss of Z_S and Z_L is greater than 35 dB, then (1) should be accurate within about 3.6%. However, in our case, the probe impedance has a 20 dB return loss. To correct for this error, a laser trimmed 500 Ω resistor is measured and used to calibrate Z_S and Z_L.

Measuring Capacitance

At frequencies well below the resonance, the resonator's impedance is capacitive with a value that is approximately equal to C_0. Thus C_0 can be extracted by performing a single frequency S-parameter measurement

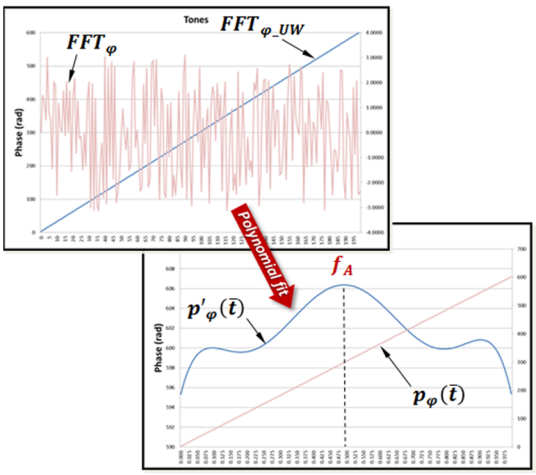

Figure 4: The generated FFT phase (radian) response, FFT_{φ}, is corrected with known phase offset, unwrapped and unwounded by 2π to derive FFT_{φ_UW}. An odd polynomial curve is fitted to the unwound phase, $p_{\varphi}(\bar{t})$, and f_A can be extracted from the polynomial derivative, $p'_{\varphi}(\bar{t})$.

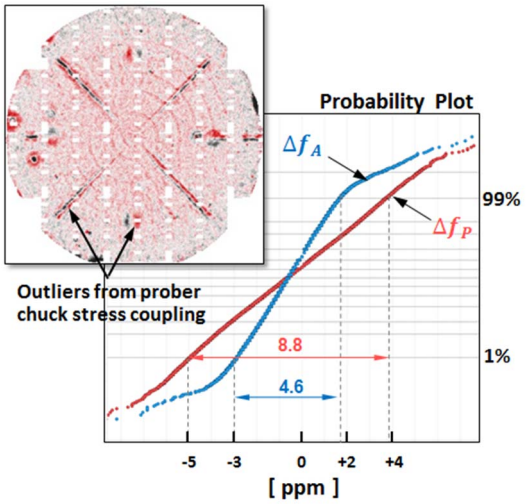

Figure 5: The probability plot of a single-wafer reproducibility test performed at 30°C. Δf_A shows tighter variation than Δf_P. The vacuum groove ring pattern and circular hot-spots are observed due to resonator being locally stressed by the prober chuck.

at 50 MHz. Since it is only done once at a single frequency, the impact on overall test time is minimal. The additional transmission line on the input and output side of the µ-resonator is de-embedded from the measurement following procedures described in [14].

The µ-resonator used in this study is a 2-pad 1-port passive device with no ground reference. It is electrically floating in this 2-port test configuration, which makes the setup more susceptible to static charge buildup in the signal path. A 1 MΩ resistor is added on the probe card to ground on each port to dissipate charge accumulation during the index time of the prober.

EXPERIMENTAL RESULTS

RF measurement errors can be introduced from calibration, measurement technique, prober chuck temperature control, probe card board design, contact resistance, etc. To evaluate this test configuration, the multi-tone technique was implemented on an Advantest V93000 with Port Scale RF using a 16-site Cascade Pyramid Probe card, and the frequency measurement error was collected and analyzed.

Repeatability and Reproducibility

Table I and Table II show the Δf_P and Δf_A repeatability and reproducibility data, respectively. These results depend on the accuracy of the RF subsystem used. During the wafer-level 100× repeatability test, all sites were tested with a constant z-height control. Whereas during the reproducibility test, the 7 wafers had a new auto-height setup between the first and the second runs. In both experiments, Δf_A had consistently lower variation than Δf_P. Therefore f_A is the preferred frequency when using multi-tone signals for the TCF calculation. As shown in the inset of Figure 5, the reproducibility outliers were coming from the capacitance and stress coupling to a standard wafer prober chuck. The vacuum groove ring pattern and circular hot-spots were observed during the Δf_P and Δf_A measurements. The ring pattern fell inside Δf_A ±5 ppm range where the hot-spots had been observed up to about 100 ppm.

The measured quality factor is within 0.1% from the values extracted from S-parameters. This measurement approach has been found to be more accurate and efficient than extractions using S-parameters. It is because the derivate calculation cancels out temperature variations in the cable group delay and other constant phase offsets in the captured signal to which S-parameter measurements are subject. When implemented on a production tester, it took about 90 minutes to finish characterizing 80,000 µ-resonators and the testing cost had been reduced by 40%.

TCF Characterization

These resonators were measured at room temperature T_0 and two additional references, preferably at the application maximum and minimum (T_H and T_L), for curve fitting to obtain their TCFs. Figure 6 records the temperature characteristic of 40 passively-compensated µ-resonators (the red data set), showing a quadratic

Table I. ATE tester repeatability data (same site, repeated 100 times)

PARA-METER	PPM (RANGE)	PPM (SIGMA)	SITES
Δf_P	5.98	1.52	16
Δf_A	2.40	0.48	16

Table II. ATE tester reproducibility data (80,000 dies per wafer, total of 7 wafers)

PARA-METER	PPM (MEDIAN)	PPM (RANGE)	PPM (SIGMA)	WAFERS
Δf_P	−0.19	8.30 – 9.35	1.82	7
Δf_A	0.09	3.85 – 6.37	0.48	7

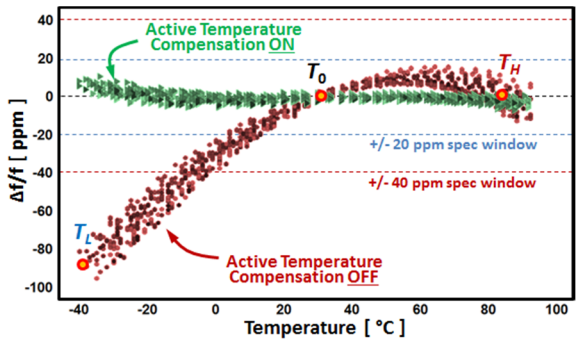

Figure 6: The TCF characteristic is accurately transferred to packaged oscillators through the 3-temperature f_A pre-screening at wafer-level. A fractional-PLL providing a step size of 0.7 ppm is used for active temperature compensation.

behavior which can be expressed by 2nd-, 1st-, and 0th-order temperature coefficients as

$$\frac{\Delta f}{f_0} \times 10^6(T) = TC_2(T - T_0)^2 + TC_1(T - T_0) + TC_0. \qquad (2)$$

Among them, TC_2 determines the "curvature" of the parabola, TC_1 defines the slope of the curve, and TC_0 indicates the initial accuracy due to process variation. TC_1 together with TC_2 also determines the turnover temperature (ToT) at which the frequency drift over temperature variation is minimum. After this three-temperature calibration, one can solve TC_2, TC_1 and TC_0 and use this information to interpolate any points on the curve for active temperature compensation. Oscillation sustaining circuits with frequency tuning function are introduced for this purpose. In this study, a fractional-PLL was assembled with the resonator die in a QFN package. When the active compensation function was turned on, the green data set demonstrated ±10 ppm frequency stability from −40°C to 85°C. A non-zero average 3rd-order coefficient in the resulting temperature curve was also observed. Nonlinearity in the temperature sensor and the µ-resonator temperature curve itself both contributed to this 3rd-order term. This effect can be further corrected with the expense of a high-resolution temperature sensor and an extra read point.

CONCLUSION

Accurate resonance frequency measurement is crucial for technology development and process monitoring of vibration-based RF MEMS devices. A production test procedure compatible with high volume micro-resonator manufacturing was presented in this paper. As the first ATE tester in Texas Instruments for the wafer-level resonator characterization, the Advantest V93000 adopted the innovative multi-tone methodology and frequency extraction techniques for TCF parameter pre-screening. By measuring the magnitude and phase changes of injected tones, µ-resonators were characterized with good accuracy yet half of the testing cost compared to conventional methods. When this configuration was implemented on a 16-site production test board, each touch down took only 0.35 seconds. With these techniques, it is shown that µ-resonators can be quickly and accurately characterized on nearly any standard production testers used in TI facility. Infrastructure using MATLAB scripts, IC-CAP, and JMP are also developed to automatically generate statistical and corner SPICE models which will be reported in our future papers.

ACKNOWLEDGEMENTS

Authors would like to thank colleagues who have contributed data for the talk and paper: Zachary Hughes, Per Roine, and Nicholas Dellas. Sincere appreciation also goes to engineers in DHC, DFAB, and DCL for their substantial efforts on this technology.

REFERENCES

[1] H. Lutz et al., "MEMS Oscillators for High Volume Commercial Applications", in *Tech. Digest of the Transducers*, 2007.

[2] H. Lee, A. Partridge, and F. Assaderaghi, "Low Jitter and Temperature Stable MEMS Oscillators", in *Tech. Digest of the IEEE IFCS*, 2012.

[3] W.-T. Hsu, "Recent Progress in Silicon MEMS Oscillators", in *Tech. Digest of the 40th Annual Precise Time and Time Interval (PTTI) Meeting*, 2008.

[4] C. T.-C. Nguyen and R. T. Howe, "CMOS Micro-mechanical Resonator Oscillator", in *Tech. Digest of the IEEE International Electronic Devices Meeting (IEDM)*, 1993.

[5] R. Ruby, J. D. Larson, P. Bradley, and Y. Oshmyansky, "Ultra-Miniature, High-Q Filters and Duplexers using FBAR Technology", in *Tech. Digest of the IEEE ISSCC*, 2001.

[6] P. Bradley et al., "A Film Bulk Acoustic Resonator (FBAR) Duplexer for USPCS Handset Applications", in *Tech. Digest of the IEEE MTT- Symposium,* 2001.

[7] R. Aigner et al., "Advancement of MEMS into RF-Filter Applications", in *Tech. Digest of the IEEE IEDM*, 2002.

[8] Q. Zou et al., "Temperature-Compensated FBAR Duplexer for Band 13", in *Proceeding of the Joint UFFC, EFTF, and PFM Symposium*, 2013.

[9] A. Tajic et al., "No-Drift BAW-SMR: Over-moded Reflector for Temperature Compensation", in *Tech. Digest of the IEEE IUS*, 2016.

[10] A. Khanna et al., "A Film Bulk Acoustic Resonator (FBAR) L Band Low Noise Oscillator for Digital Communications", in *Tech. Digest of the 32nd European Microwave Conference (EuMC)*, 2002.

[11] S. Gilbert et al., "Manufacturing and Reliability of Chip-scale Packaged FBAR Oscillators", in *Tech. Digest of the IEEE IUS*, 2014.

[12] S. Sridaran et al., "Low Jitter FBAR Based Chip Scale Precision Oscillator", in *Tech. Digest of the IEEE IUS*, 2014.

[13] https://www.cmicro.com/products/probe-cards

[14] "De-embedding and Embedding S-parameter Networks Using a Vector Network Analyzer," Agilent Application Note 1364-1.

CONTACT

*E. Yen, tel: +1-669-7213522; ernest.ttyen@ti.com